



HAL
open science

Fast carbonylation reaction from CO₂ using plasma gas/liquid microreactors for radiolabeling applications

Marion Gaudeau, Mengxue Zhang, Michaël Tatoulian, Camille Lescot,
Stéphanie Ognier

► To cite this version:

Marion Gaudeau, Mengxue Zhang, Michaël Tatoulian, Camille Lescot, Stéphanie Ognier. Fast carbonylation reaction from CO₂ using plasma gas/liquid microreactors for radiolabeling applications. *Reaction Chemistry & Engineering*, 2020, 5 (10), pp.1981-1991. 10.1039/D0RE00289E. hal-03082012

HAL Id: hal-03082012

<https://hal.science/hal-03082012>

Submitted on 13 Jan 2021

HAL is a multi-disciplinary open access archive for the deposit and dissemination of scientific research documents, whether they are published or not. The documents may come from teaching and research institutions in France or abroad, or from public or private research centers.

L'archive ouverte pluridisciplinaire **HAL**, est destinée au dépôt et à la diffusion de documents scientifiques de niveau recherche, publiés ou non, émanant des établissements d'enseignement et de recherche français ou étrangers, des laboratoires publics ou privés.

Fast carbonylation reaction from CO₂ using plasma gas/liquid microreactors for radiolabeling applications[†]

Marion Gaudeau^a, Mengxue Zhang^a, Michael Tatoulian^a, Camille Lescot^{b*}, Stéphanie Ognier^{a*}

Carbon-11 is undoubtedly an attractive PET radiolabeling synthon because carbon is present in all biological molecules. It is mainly found under ¹¹CO₂, but the latter being not very reactive, it is necessary to convert it into a secondary precursor. ¹¹CO is an attractive precursor for labeling the carbonyl position through transition-metal mediated carbonylation because of its access to a wide range of functional groups (e.g., amides, ureas, ketones, esters, and carboxylic acids) present in most PET tracer molecules. However, the main limitations of ¹¹CO labeling are the very short half-life of the radioisotope carbon-11 and its low concentration, and the low reactivity and poor solubility of ¹¹CO in commonly used organic solvents. In this work, we show that a possible solution to these limitations is to use microfluidic reactor technology to perform carbonylation reactions, whilst a novel approach to generate CO from CO₂ by plasma is described. The methodology consists of the decomposition of CO₂ into CO by non-thermal DBD plasma at room temperature and atmospheric pressure, followed by the total incorporation of CO thus formed in the gas phase by carbonylation reaction, in less than 2 min of residence time. This “proof of principle” developed in carbon-12 would be further applied in carbon-11. Although considerable advances in ¹¹CO chemistry have been reported in recent years, its application in PET tracer development is still an area of work in progress, because of the lack of commercially available synthesis instruments designed for ¹¹C-carbonylations. To the best of our knowledge, such an innovative and efficient process, combining microfluidics and plasma, allowing the very fast organic synthesis of carbonyl molecules from CO₂ with high yield, in mild conditions, has never been studied.

Introduction

Positron emission tomography (PET) is a powerful non-invasive imaging technique that uses radiolabeled compounds as molecular probes to image biological processes *in vivo*, for research and clinical diagnostic¹. These imaging probes are labeled with short-lived radioisotopes (e.g., ¹⁸F, ¹¹C, ¹³N, ¹⁵O). Its rising use in recent years has increased the demand for the development of new PET tracers and that of new synthetic methods for these tracers.

Carbon-11 is a valuable positron-emitting radionuclide, because carbon is the main constituent of all biological molecules². However, due to the very short half-life time of ¹¹C ($t_{1/2} = 20.4$ min), the synthesis of ¹¹C-labeled radiotracers is not without challenge: chemists must find rapid synthesis routes so that the labeled molecule can be produced and isolated within two half-lives, i.e. 40 min for ¹¹C.

As carbon-11 mainly comes from ¹¹CO₂ generated in biomedical cyclotrons³, it is crucial to have a method allowing the rapid radiolabeling of molecules directly from ¹¹CO₂. However, considering the high stability of CO₂, it is necessary to envisage the transformation *in situ* of ¹¹CO₂ into a more reactive species. Among the existing carbon-11 radiolabeling methods, carbonylation reactions with ¹¹CO are of great interest since it leads to a wide range of functional groups (amides, ketones, ureas, esters, lactones, carboxylic acids, ...) having interesting pharmaceutical properties^{4–12}. These functional groups are thus

present in many biologically interesting compounds, and more specifically the amide function obtained by aminocarbonylation^{13–16}.

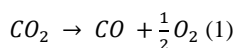
Our objective is to develop an original process of introducing a carbon atom through aminocarbonylation using CO₂ as carbon source. The development will be performed with carbon-12 with the vision of future use in radiolabeling with carbon-11, so taking into account the time constraint and the security issues related to the radioactive nature of carbon-11.

Considering these parameters, carbonylation reactions usually require the use of intensified processes to ensure a high reaction rate. As for the gas-liquid reaction, high pressure autoclave reactors generating high partial pressures of CO have proven to be effective for ¹¹C radiolabeling¹⁷, but these devices are expensive and require special safety precautions. Another way to intensify the process is to use microreactors^{18–31}. Indeed, the large surface area to volume ratio of microfluidic systems improves the gas-liquid mass transfer between the flow of gas containing CO and the liquid phase reagent, leading to efficient carbonylation reactions with a short residence time³². Improved transfer in microreactors also induces milder reaction conditions compared to conventional methods, and their small volume is perfectly suited to the manipulation of sub-micromolar amounts of radioactive reagents.

Concerning the reduction of CO₂ to CO, carbon dioxide is kinetically and thermodynamically stable³³, and therefore requires significant energy or powerful catalysts for its chemical transformation. Several methods can be used for the splitting of CO₂ into CO (chemical, electrochemical, photochemical)^{10–15,34–45} but plasma has been demonstrated as an effective and clean way^{46,47}. Indeed, under electric discharges, the highly energetic

species (excited neutrals, radicals, metastables, photons...) and electrons generated (with energy of [1-10] eV⁴⁸) in the plasma can break the C-O bond (2.9 eV/molecule at 300 K) and transform CO₂ molecules. Compared to classical routes, the conversion of CO₂ by plasma does not generate waste and is an "atom-economical" approach without the use of catalysts and reducing agents.^{16,49–51}

Despite the complex plasma chemistry of the reaction, the splitting of CO₂ can be summarized as follows:

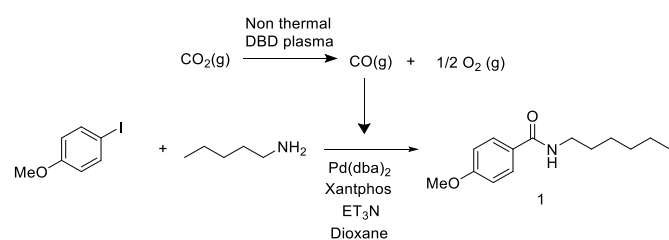


$$\Delta H_R = 2.9 \text{ eV/molecule at } 300\text{K} = 280 \text{ kJ/mol}$$

Among the different plasma systems, non-thermal (or cold) atmospheric plasma appears as a convenient and innovative method, since it is easy-to-handle and is operated under mild conditions (room temperature, atmospheric pressures)⁵². One of the most exploited non-thermal plasma configurations for CO₂ splitting is the dielectric barrier discharge (DBD), for which one or two dielectric layers are inserted between the electrodes. It prevents the formation of electric arcs detrimental to the device integrity and allows homogenous discharges in the discharge gap. Simple to use and to scale up, the DBD configuration is a promising technique for the CO₂ conversion to CO at industrial scales⁵³.

Thus, the combination of microfluidics and plasma seems to be an ideal solution for carrying out the rapid carbonylation reactions required for ¹¹C radiolabeling for PET.

Here we propose a new method to synthesize carbonylated molecules starting from CO₂ directly, associating microfluidics and plasma, within a very short residence time (several minutes) and under mild conditions. The proposed system is composed of two microreactors in a continuous 2-step process for the carbonylation reaction starting from CO₂: a first plasma microreactor for the CO₂ splitting and a second gas-liquid microreactor for the carbonylation reaction. To evaluate the efficiency of this innovative process combining plasma and microfluidics, aminocarbonylation of p-iodoaniline and n-hexylamine in the presence of a palladium catalyst to form N-hexyl-4-methoxybenzamide (**1**) has been chosen as proof-of-concept because of its high selectivity and efficiency to trap CO. Furthermore the reaction mixture is easy to analyse by ¹H NMR¹⁶. This process would subsequently be applied to radiolabeling with carbon-11. To the best of our knowledge, such a fast and efficient process, starting from CO₂ leading to amide in mild conditions, has never been studied. Scheme 1 presents the general reaction scheme.



Scheme 1: General reaction scheme

Experimental

The study of the decomposition of CO₂ into CO by plasma and the study of aminocarbonylation reaction have firstly been carried out separately in two separate microreactors, then the two microreactors were coupled in line for the 2 steps synthesis.

Microreactors

Two glass microreactors with identical geometry have been used in this study: one with metallic electrodes for the plasma reactor and the other without electrodes for the carbonylation reaction. The patented reactor geometry has been previously developed in our group⁵⁴ and demonstrated efficient for gas-liquid reactions^{55–57}. The reactor has been designed to provide a stabilized gas-liquid parallel flow in 1-m long channel. The gas flows in the central channel, while the liquid phase flows in the two side channels along the gas phase (Figure 1a and Figure 3). The internal volume of the gas phase is 10 μL and that of the liquid phase is 25 μL.

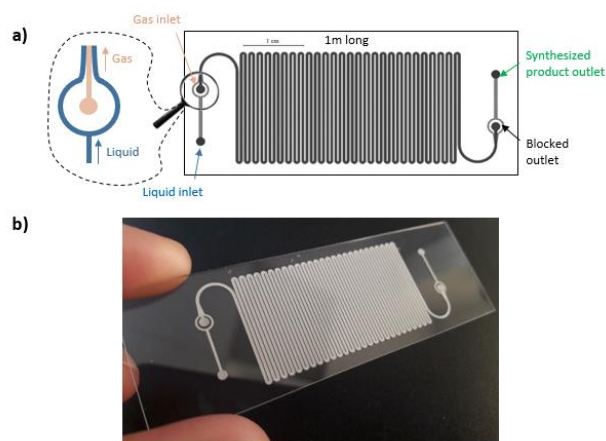


Figure 1: a) Top-view of the channel. b) Picture of the glass microreactor

Aminocarbonylation

Material

The liquid phase was prepared by mixing in the following order: 0.0125 mmol of Pd(dba)₂ [Bis(dibenzylideneacetone)palladium(0)] (5 mol%), 0.025 mmol of Xantphos [4,5-bis(diphenylphosphino)-9,9-dimethylxanthene] (10 mol%), 0.25 mmol of p-iodoaniline (1 eq), 3 mL of Dioxane, 0.5 mmol of n-hexylamine (2 eq), 0.5 mmol of trimethylamine (2 eq).

Fluidic set up

A biflow reactor was used for the aminocarbonylation reaction (Figure 1b). Details about the connectors assembling are given in Electronic Supplementary Information (ESI). Pure CO from commercial CO cylinder has been used for this part and was managed by means of mass flow controller (Bronkhorst EL-FLOW PRESTIGE FG-201CV) in the range of 0.014 – 4 sccm. The liquid flows were controlled by a syringe pump (kdScientific Legato 180) in the range of 7.5 – 20 μL/min. The liquid phase was introduced through the liquid inlet and the gas phase through the gas inlet. In both cases, the respective flowrate of

each phase determines its residence time in the chip. One of the reactor outlets was sealed while the other outlet of the microreactor was connected to a vial for liquid collection.

TEMPERATURE CONTROL

An infrared lamp (Bioseb Lab Instruments) was used to heat the microreactor, and the temperature was controlled by two thermocouples: one was fixed below the microreactor (Figure 2b), and the other above. The temperature inside the microreactor was determined supposing that the temperature changes linearly between the top and the bottom of the reactor. During the experiments, the typical temperature difference between the bottom and the top of the reactor was about 10 °C. The operating temperature was controlled in the range of 20 – 80 °C by adapting the distance from the IR lamp.

Flow characterisation

The chip was placed under a microscope (Leica Z16 APO, Germany) onto which was mounted a CCD camera (PixelLINK PL-B781U) for flow visualisation, with the chip being back-illuminated by a diffuse LED lamp. Figure 3 shows the gas-liquid flow inside microchannel through the CCD camera. A stable gas-liquid flow was observed in all the tested conditions.

Liquid analysis

The liquid was collected at the outlet in a vial during 45 min. Conversion of p-iodoanisole into the amide **1** was determined by crude ¹H NMR analysis (CDCl₃) without internal standard, by comparing to the remained p-iodoanisole quantity* (see also ESI).

Each experiment was conducted at least twice, and the presented results correspond to the average of the measured substrate conversions. An error of 5% is appreciated on NMR results. The limit of detection of NMR spectroscopy is 5-10%, that is why the result >90% was given when no more trace of starting material was detected.

Cleaning

Prior to the reaction, the reactor was initially rinsed by a stable dioxane-CO flow during 30 min with the reactor temperature well controlled. Then, the dioxane syringe was replaced by a syringe containing the reaction liquid phase, and the reaction was carried out, collecting the solution from the outlet of the microreactor in a new vial (synthesized product vial). After the reaction, the reactor was thoroughly rinsed again with a stable dioxane-CO flow for 15 minutes.

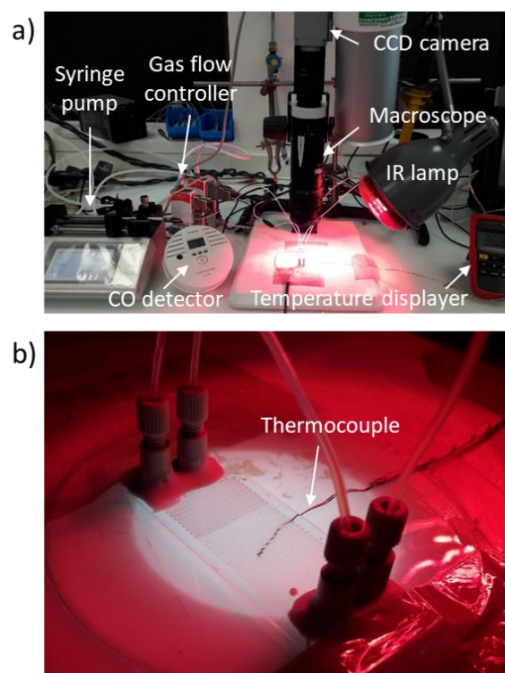


Figure 2: a) Picture of the entire installation; b) Microreactor being back-illuminated by a diffuse LED lamp, with thermocouple below (thermocouple above does not appear on this picture)

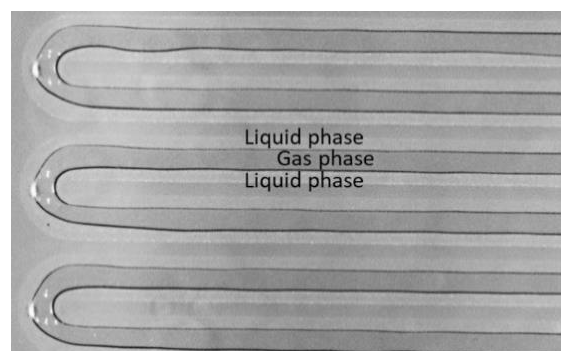


Figure 3: Picture of microchannel from the camera

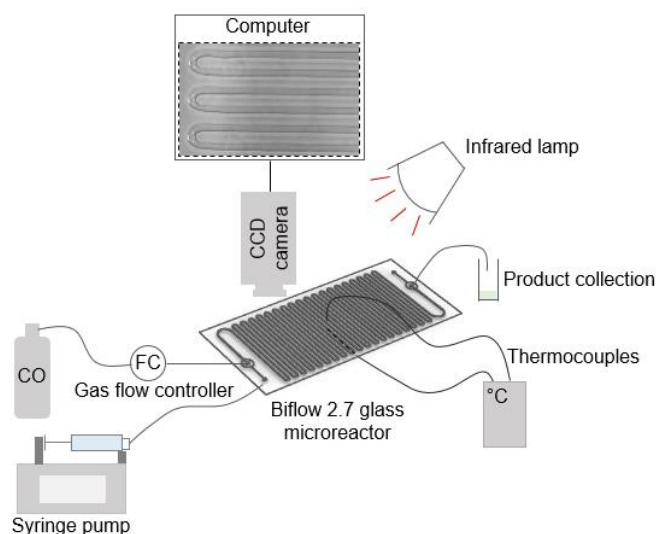


Figure 4: Experimental set-up used for aminocarbonylation reaction

Decomposition of CO₂ into CO by DBD plasma

Microreactor & Fluidic set up

A biflow reactor with combed-shaped copper electrodes was used for the CO₂ splitting. The microreactor was coated of PDMS (PolyDiMethylSiloxane) to avoid parasite discharges outside of the reactor. Details about electrodes deposition and reactor assembly are given in Electronic Supplementary Information (ESI). A such configuration corresponds to a double-DBD configuration, with two dielectric layers (glass) protecting the electrodes from direct contact with the plasma. This configuration prevents electrodes degradation which could shorten electrodes' lifetime and may introduce metallic nanoparticles into the reactive system. A mixture of CO₂ and Ar has been used in our experiments, since the addition of argon leads to a higher conversion of CO₂ to CO^{58,59}, due to a reduction in the plasma breakdown voltage, and a charge exchange with Ar⁺ argon ions increasing the CO₂⁺ population. The mixture of Ar and CO₂ via a T-mixer was managed by mass flow controllers (Bronkhorst EL-FLOW PRESTIGE FG-201CV) in the range of 0.125 – 0.25 sccm for CO₂ and 2.25 – 2.375 sccm for Ar, to one of the inlets of the reactor, while the other was sealed. One of the reactor outlets was sealed while the other outlet was connected to a gas sampling bulb. The outlet of the bulb was connected to a bubble flowmeter for a regular flowrate control during the experiment, ensuring the absence of leakage.

Electrical set up

A sine wave signal (AC) was sent from a function generator (ELC, GF467F, 5MHz) to a voltage amplifier (TREK 10/40A high voltage amplifier ×1000) which multiplies the input voltage by 1000. This high voltage was applied to the microreactor and a 3.11 nF capacitor in series and was monitored with an oscilloscope (PicoScope 5000 Series) through the 1000:1 outlet of the amplifier. The capacitor was used to obtain discharge electric charge necessary to calculate the discharge power, and the capacitance voltage was measured via a low voltage probe (Teledyne LeCroy PP024 500 MHz 10:1). The frequency used was between 1000 and 3000 Hz, and the high voltage was between 9 and 18 kVpp. Figure 5 shows the diagram of the experimental setup.

Power assessment

The measurement of the discharge power supplied to the microreactor was determined using the Lissajous method and is described in ESI. The corresponding standard deviation of the calculated power lies below 3%.

Gas analysis

After 20 minutes' reaction (necessary time for the system to achieve the steady state), the gas leaving the microreactor was collected from the bulb with a syringe and was injected into an

Agilent Technologies 490 Micro GC equipped with two columns (column PoraPLOT U, 10 meters long with heated injector, and column Molesieve 5A with backflush capability and heated injector) and micro-machined Thermal Conductivity Detector (TCD). Calibrations were made for CO/Ar and CO₂/Ar mixtures distinctly with mixtures of known compositions. Each experiment was conducted three times.

Temperature measurement

A thermocouple was positioned under the reactor (blue cable on Figure 6) to measure the temperature at the surface of the bottom PDMS layer. The temperature inside microchannels was supposed to be equal to this temperature, thus neglecting the thermal resistances of the PDMS coating and the glass slide relatively to the convection boundary layer. The temperature was recorded once stabilized.

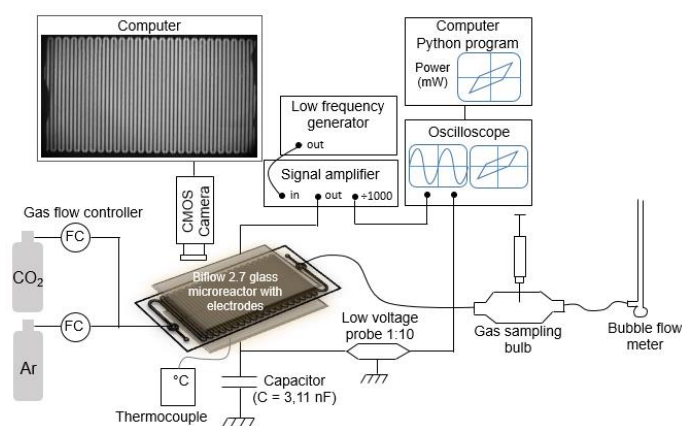


Figure 5: Experimental set-up for CO₂ splitting reactions

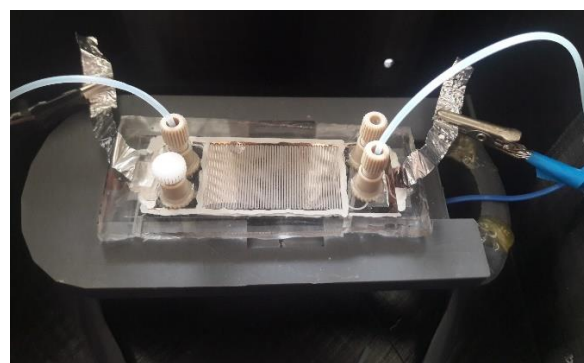


Figure 6: Picture of the plasma microreactor with fluidic connections and electrical connections, and thermocouple in contact with the bottom PDMS layer surface

Coupling

The two microreactors previously described were set in line to carry out the aminocarbonylation from CO₂. In the first microreactor, the decomposition of CO₂ into CO by plasma was achieved as explained above, and the outlet gas mixture was introduced directly into the second microreactor along with the liquid phase for aminocarbonylation reaction.

The second microreactor was heated to the appropriate temperature with IR lamp and thermocouples, and the gas-liquid flow was observed by the CCD camera, as explained before. The cleaning protocol was similar to that used for aminocarbonylation reaction prior and after the reaction. The liquid was collected at the outlet of the second reactor during 45 min. The collected liquid was analysed by ^1H NMR spectroscopy.

Results & discussion

Aminocarbonylation from commercial CO

Aminocarbonylation reaction was first studied using commercially available CO in order to find the optimized conditions leading to a maximum conversion of substrate into amide **1**.

Optimization of the temperature

In a first time, the reaction temperature was optimized, starting from 80°C which was the reaction temperature in batch process according to C. Lescot et al.¹⁶. All the reactions were performed with a liquid flowrate of 10 $\mu\text{L}/\text{min}$, corresponding to a liquid residence time of 60 seconds, and a CO flowrate of 1.5 sccm. Under these conditions, the CO was in excess, the molar ratio between CO and the substrate being 80. Results are shown in Table 1. A full conversion was obtained for temperatures above 50°C (Table 1, entries 1 - 4). Reducing the reaction temperature to 40°C and 30 °C resulted in conversions of 81% and 76% respectively (Table 1, entries 5 and 6). Finally, 56% conversion was obtained at room temperature (Table 1, entry 7).

The optimized temperature was then found to be 50°C with a full conversion after 60 s residence time (Table 1, entry 4). To compare with the batch process (details in ESI), only 41% conversion was obtained for a reaction time of 45 min at 50°C. The better result obtained in microfluidic conditions can be explained by the intensified gas/liquid transfer thanks to the very large surface area to volume ratio. In all that follows, the temperature was set to 50°C.

Optimization of the liquid residence time

The liquid residence time is a key parameter in this study, as the aminocarbonylation reaction takes place in the liquid phase. The liquid residence time is calculated by dividing the volume of the liquid phase in the microreactor by the liquid flowrate. The residence time of the liquid was varied by changing the liquid flowrate. The CO flowrate was adjusted to keep the stable gas/liquid flow inside microchannels.

Starting from previously optimized parameters (Table 2, entry 1), the liquid residence time was reduced to 40 s by increasing the liquid flowrate to 15 $\mu\text{L}/\text{min}$, and a full conversion was still obtained (Table 2, entry 2). Reducing further the liquid residence time to 30 s resulted in a 62% conversion (Table 2, entry 3). This low conversion may be explained by the residence time which is too short to allow the reaction to reach completion. Hence, the optimized liquid residence time was 40

s corresponding to a liquid flowrate of 15 $\mu\text{L}/\text{min}$, and has been kept thereafter.

The CO flowrate was slightly reduced to 2.5 sccm, leading to full conversion. With these conditions, a 95% isolated yield of amide **1** was obtained.

Study of the CO volume concentration in the gas phase

Then, the influence of CO volume concentration in the gas phase was studied in order to be both in conditions close to the actual coupling conditions where the conversion of CO_2 to CO by plasma is low, but also close to radiolabeling conditions where $^{11}\text{CO}_2$ is diluted in low concentration in a carrier gas. Ar/CO mixtures of various CO volume concentrations in the gas phase (100%, 5.6%, 1.1%, and 0.6%) were injected while the total gas flowrate was maintained at 2.5 sccm and the liquid flowrate was 15 $\mu\text{L}/\text{min}$. These CO volume concentrations corresponded to CO to substrate molar flow ratio $F_{\text{CO}}/F_{\text{SUBSTRATE}}$ of 89, 5, 1 and 0.5 respectively. Calculation details are given in ESI. The results are shown in Table 3. The reaction with previous optimized parameters corresponds to a CO volume concentration of 100% and a CO to substrate molar flow ratio $F_{\text{CO}}/F_{\text{SUBSTRATE}}$ of 89 (Table 3, entry 1). The results indicate that the conversion decreases by decreasing the CO volume concentration, because of the decreasing quantity of CO entering the liquid phase. Despite the CO excess, the conversion for $F_{\text{CO}}/F_{\text{SUBSTRATE}} = 5$ was not complete, and can be explained by slower kinetics, either because the mass transfer is slower or because the intrinsic kinetics of the reaction are slower. On the other hand, the result at 1.1% CO volume concentration (Table 3, entry 3) was very promising for the future, because despite the low conversion of CO_2 into CO by plasma, a good conversion of the substrate into the amide **1** can be expected for coupling.

Influence of the liquid residence time in equimolar conditions

Keeping a CO volume concentration of 1.1% ($F_{\text{CO}}/F_{\text{SUBSTRATE}} = 1$), the influence of the liquid residence time on the substrate conversion was studied by varying the liquid flowrate (3rd column, Table 4). The total gas flowrate was also adjusted in order to ensure a stable gas-liquid flow (4th column, Table 4), while the CO volume concentration was fixed at 1.1% in the CO/Ar mixture. CO was supplemented with argon (6th column, Table 4) to reach the total gas flowrate. Calculation details about flowrates, and the estimation of pressure drop (5th column, Table 4) and CO partial pressure (6th column, Table 4) are given in ESI.

Contrary to what we could expect, conversion decreases with the liquid residence time. This unexpected result can be explained by the decrease, even moderate, of the CO partial pressure. Indeed, to increase the liquid residence time from 40 to 80 seconds, the gas and liquid flowrates were decreased, leading to a decrease of the inlet pressure, and therefore the CO partial pressure at the reactor inlet. For example, the partial pressure of CO at the reactor inlet decreases by roughly 25% when the liquid residence time was multiplied by a factor 2. Hence, this decrease of CO partial pressure could explain the decrease of substrate conversion, as less CO was transferred to

the liquid phase. Those results suggest that the CO diffusion at the gas/liquid interface can be a hindering step for reactions under low pressure conditions, contrary to the work of Jensen et al.⁶⁰ where reactions are conducted with high CO pressures

(2.8 – 13.8 bars) that suggest that the oxidative addition was the rate-limiting step below 120°C.

Entry	Temperature (°C) [error +/- 1°C]	Conversion of p-iodoanisole into amide 1 (%)	Standard deviation (%) [†]
1	80	>90	0
2	70	>90	0
3	60	>90	0
4	50	>90	0
5	40	81	± 14
6	30	76	± 8
7	20	56	± 8

Table 1: Optimization of temperature, for a 10 μL/min liquid flowrate and 1.5 sccm CO flowrate

[†] Standard deviation calculated from the different measured substrate conversions obtained for the same experimental conditions

Entry	Liquid flowrate (μL/min)	Liquid residence time (s)	CO flowrate (sccm)	Conversion of p- iodoanisole into amide 1 (%)	Standard deviation (%)
1	10	60	1.5	>90	0
2	15	40	3.0	>90	0
3	20	30	4.0	62	± 4

Table 2: Optimization of the liquid residence time, at 50°C

Entry	CO volume concentration (%)	$\frac{F_{CO}}{F_{SUBSTRAT}}$	Conversion (%)	Standard deviation (%)
1	100	89	90	± 7
2	5.6	5	61	± 7
3	1.1	1	53	± 10
4	0.6	0.5	14	± 3

Table 3: Study of CO volume concentration with a total gas flowrate of 2.5 sccm gas residence time < 1s, and 15 μL/min as liquid flowrate (liquid residence time = 40 s), at 50°C

Entry	Liquid residence time (s)	Liquid flowrate (μL/min)	Total gas flowrate (sccm)	Inlet experimental partial pressure of CO (mbar)	Conversion (%)	Standard deviation (%)
1	40	15	2.5	21	53	± 10
2	60	10	1.8	17	33	± 3
3	80	7.5	1.3	16	30	± 11

Table 4: Influence of the liquid residence time in equimolar conditions at 50°C, CO volume concentration = 1.1%

Comparing Table 2 and Table 4, it can be concluded that the influence of the liquid residence time on the substrate conversion depends on the percentage of CO in the gas mixture: if the CO is in excess in regard to the substrate, the conversion increases with the residence time (Table 12), on the other hand, if the CO is not abundant supply, the increase of the residence time can negatively affect the conversion because of the influence of the gas flowrate on the CO inlet partial pressure (Table 4).

Aminocarbonylation from CO resulting from the splitting of CO₂ by DBD plasma

Determination of plasma parameters

In the previous part, it has been shown that, using a gas-liquid microreactor, it is possible to obtain good conversions with CO volume concentrations in the gas phase as low as 1%. The objective of this second part is to find operating conditions allowing the production of such CO volume concentrations from CO₂ splitting using a plasma DBD microreactor. In this part, the liquid and gas flowrates are fixed at 15 μL/min and 2.5 sccm respectively.

The decomposition of CO₂ into CO by DBD plasma was studied with CO₂/Ar mixtures of 10/90 and 5/95 volume ratios. Indeed, Ramakers and al. showed that addition of Ar led to higher CO₂ conversions, and the effect was more pronounced for Ar fractions above 70%⁵⁸.

For each gas mixture, various plasma parameters (voltage, frequency) were used to vary Specific Energy Input (SEI), defined as the ratio of the discharge power to the gas flow rate:

$$SEI\left(\frac{J}{mL}\right) = \frac{Power\ (W)}{total\ flowrate\ \left(\frac{mL}{min}\right)} \times 60\left(\frac{s}{min}\right)$$

The specific energy input is generally considered as the characteristic parameter of the plasma discharge.

The influence of the SEI on the reactor temperature, the CO volume concentrations at the outlet and the CO₂ conversion were studied for each gas composition.

Temperature

The reactor temperature was monitored with the thermocouple. It can be observed that the reactor temperature increased linearly with SEI for a given gas composition, while the temperature never exceeded 60 °C. The temperature is moderate because of fast dissipation of the low amount of heat generated by the plasma thanks to the high surface to volume ratio of the microreactor.

CO₂ conversion

The CO₂ conversion is defined as the change in CO₂ concentration over the initial CO₂ concentration.

$$X_{CO_2\ abs}(\%) = \frac{\%CO_2\ INLET - \%CO_2\ OUTLET}{\%CO_2\ INLET} \times 100$$

Where %CO₂ INLET and %CO₂ OUTLET represent the volume concentration of CO₂ (in %) before applying plasma discharge and the volume concentration of CO₂ (in %) at the outlet of the reactor after 20 min run, respectively. %CO OUTLET represents the volume concentration (in %) of CO produced at the outlet of the reactor.

In Figure 8, CO₂ conversion is plotted according to SEI. For both gas mixtures, increasing SEI led to an increase in the conversion of CO₂. Increasing input power could effectively enhance the electrical field, electron temperature, electron density and gas temperature in the discharge, which contributes to the improvement of CO₂ conversion. However, the CO₂ conversion with SEI was higher for the 5% CO₂ mixture in comparison with the 10% CO₂ mixture. This is what is generally reported in the literature.⁵⁸ There are 2 possible explanations: firstly, the more argon there is, the more the dielectric strength of the gas mixture decreases, which makes it possible to benefit a greater amount of energy available for the dissociation of CO₂; secondly, the charge and energy transferred from excited Ar species to CO₂ molecules increase with a higher Ar content and there was a higher chance for the CO₂ molecule to collide with radicals or excited Ar.

CO volume concentration

In Figure 9, the CO volume concentration (in %) produced by the decomposition of CO₂ is plotted as a function of the SEI. We can observe that the CO volume concentration increased when SEI increased for the gas mixture with 10% CO₂ in Ar, but remained

almost constant for the gas mixture with 5% CO₂ in Ar. Although the increase of the Ar ratio has a positive impact on the conversion of CO₂ as we observed previously, it can also have a limiting effect as we can see here. Indeed, we can suppose that the charge transfer process between the Ar⁺ or Ar²⁺ ions and CO₂ (Ar⁺ + CO₂ → Ar + CO₂⁺), followed by the dissociative electron-ion recombination of the CO₂⁺ ions (CO₂⁺ + e⁻ → CO + O), is limited if the amount of CO₂ decreases, and so Ar⁺ or Ar²⁺ ions are less likely to meet CO₂ molecules to produce CO. A maximum percentage of CO of 1.6% ±0.4%, corresponding to a CO yield of 16%, was obtained for 10% CO₂ in Ar with a frequency of 3 kHz and a voltage of 12 kVpp. In these conditions, the conversion of CO₂ was equal to 17.0% ±5.7%, that is approximately equal to the CO yield and assume that the production of other carbon containing products is negligible. The temperature was around 42°C, and the discharge power was around 300 mW.

The CO volume concentration was determined by means of a calibration previously done on the μGC using very low CO flowrates to have a wide range of CO volume concentrations, which can imply uncertainties on the flowrates. This could explain the high uncertainties of the results here.

In the previous study of aminocarbonylation from commercial CO, we obtained 53% conversion for a CO volume concentration of 1.1%. So, the maximum CO volume concentration of 1.6% ±0.4% obtained from the decomposition of CO₂ by plasma should be enough to carry out successfully the aminocarbonylation reaction in line.

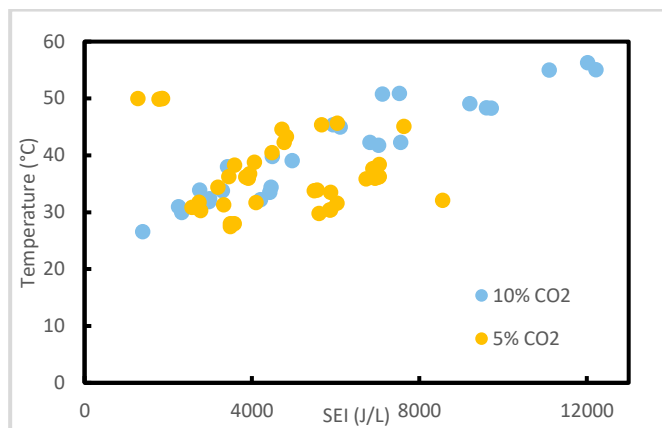


Figure 7: Graph of the temperature as a function of the SEI

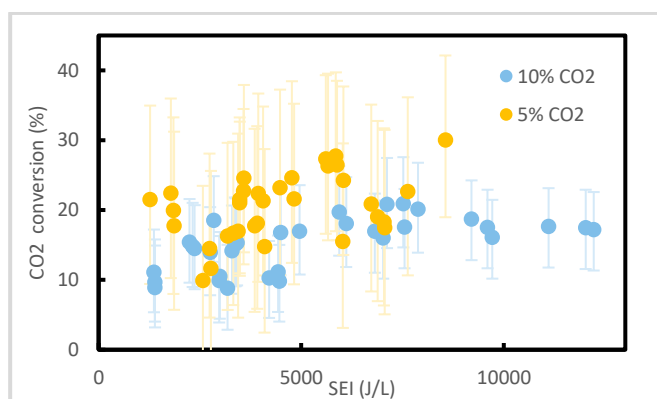


Figure 8: Graph of the CO₂ conversion as a function of the SEI

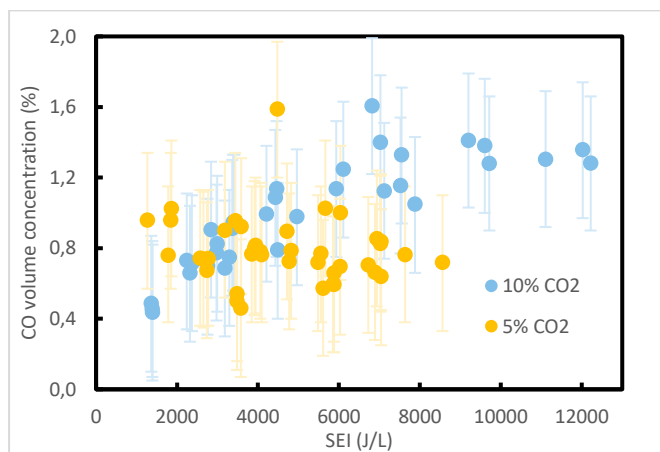


Figure 9: Graph of the CO volume concentration at the outlet as a function of the SEI

Splitting of CO₂ by DBD plasma coupled with aminocarbonylation in line

The two microreactors were assembled (Figure 10) to carry out the aminocarbonylation reaction with CO synthesized in situ from decomposition of CO₂ by plasma. The first microreactor was dedicated to the decomposition of CO₂ into CO by plasma, and the experimental conditions were a total gas flowrate of 2.5 sccm composed by CO₂/Ar mixture of 10/90 volume ratio, 3 kHz and 12 kVpp. The out-flowing gas moved into the second microreactor, in which the aminocarbonylation takes place, with a liquid flowrate of 15 μL/min at 50°C. This reaction was performed twice, and 70% conversion of the substrate into amide **1** was obtained each time. This result is closed to conversions obtained using commercial CO at similar low CO concentrations (Table 3, entry 2 & 3), the liquid residence time being 40 s for both cases. For the first time, aminocarbonylation was performed from CO₂ using a 2-step microfluidic synthesis, within a total residence time shorter than 1 min.

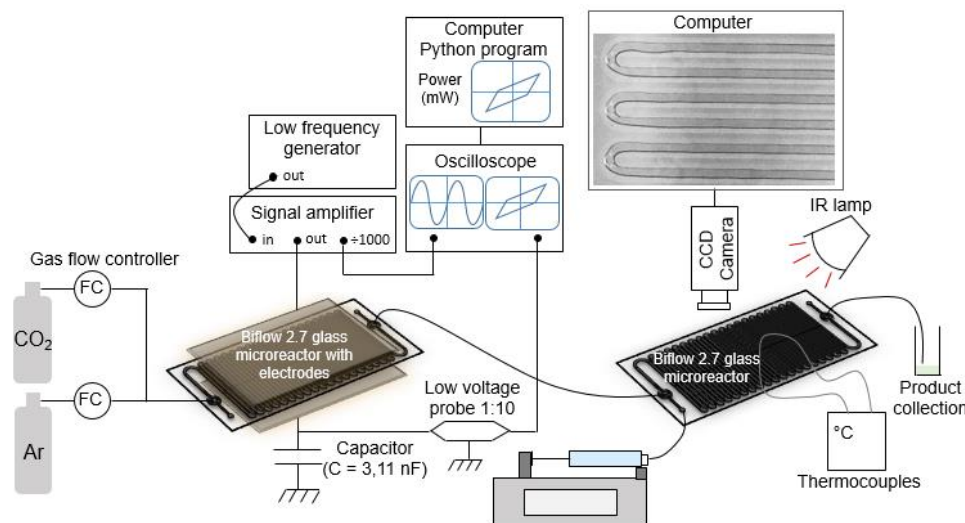


Figure 10: Experimental set-up for coupling synthesis

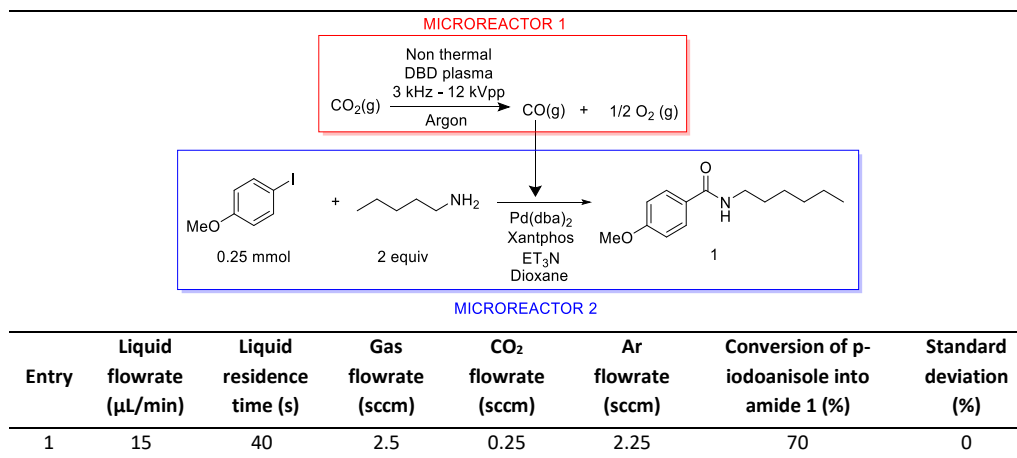


Table 5: Results of aminocarbonylation from CO produced by the splitting of CO₂

Conclusion and outlooks

In this work, amide **1** was synthesized from CO₂ with high yield, under mild conditions, thanks to an innovative process combining microfluidics and plasma. This innovative process could also be used to carry out other carbonylation reactions, and could be transferred in carbon-11 chemistry for carbon-11 radiolabeling for PET. The combination of plasma and microfluidics allows to reach a very short total process time and the radiolabeling process is no longer limited by the very short half-life of carbon 11, while keeping milder conditions compared to conventional methods. The ¹¹C-labeled-carbonylative molecules could be synthesized, purified and analysed in less than 40 min without making any compromise

between radiochemical yield (RCY) and radioactive decay. Such a process of carbonylation starting from CO₂, leading to this high substrate conversion with such mild conditions, is unprecedented in the literature and exceeds the limitations encountered so far. In addition to the radiolabeling application, the synthesis *in-situ* of CO is a real advantage for safety constraints since the CO is not being directly handled.

Conflicts of interest

There are no conflicts to declare.

Acknowledgements

This work has received the support of "Institut Pierre-Gilles de Gennes" (laboratoire d'excellence, "Investissements d'avenir" program ANR-10-IDEX-0001-02 PSL and ANR-10-LABX-31; équipement d'excellence, "Investissements d'avenir" program ANR-10-EQPX-34).

Notes and references

$$I \text{ Substrate conversion (\%)} = \frac{A}{B}$$

where A is the area of the peak of methoxy group of amide **1** (at 3.81 ppm) and B is the area of the peak of methoxy group of amide **1** (at 3.81 ppm) + the area of the peak of methoxy group of p-iodoanisole (at 3.75 ppm)

- 1 P. W. Miller, N. J. Long, R. Vilar and A. D. Gee, *Angew. Chem. Int. Ed.*, 2008, **47**, 8998–9033.
- 2 G. Antoni, T. Kihlberg and B. Långström, in *Handbook of Radiopharmaceuticals*, John Wiley & Sons, Ltd, 2005, pp. 141–194.
- 3 B. H. Rotstein, S. H. Liang, M. S. Placzek, J. M. Hooker, A. D. Gee, F. Dollé, A. A. Wilson and N. Vasdev, *Chem. Soc. Rev.*, 2016, **45**, 4708–4726.
- 4 O. Itsenko and B. Långström, *J. Org. Chem.*, 2005, **70**, 2244–2249.
- 5 B. Långström, O. Itsenko and O. Rahman, *J. Label. Compd. Radiopharm.*, 2007, **50**, 794–810.
- 6 C. Taddei and V. W. Pike, *EJNMMI Radiopharm. Chem.*, 2019, **4**, 25.
- 7 O. Rahman, *J. Label. Compd. Radiopharm.*, 2015, **58**, 86–98.
- 8 S. Kealey, A. Gee and P. W. Miller, *J. Label. Compd. Radiopharm.*, 2014, **57**, 195–201.
- 9 J. Eriksson, G. Antoni, B. Långström and O. Itsenko, *Nucl. Med. Biol.*, DOI:10.1016/j.nucmedbio.2020.02.005.
- 10 G. Buscemi, P. W. Miller, S. Kealey, A. D. Gee, N. J. Long, J. Passchier and R. Vilar, *Org. Biomol. Chem.*, 2011, **9**, 3499.
- 11 P. J. Riss, S. Lu, S. Telu, F. I. Aigbirhio and V. W. Pike, *Angew. Chem. Int. Ed.*, 2012, **51**, 2698–2702.
- 12 C. Taddei and A. D. Gee, *J. Label. Compd. Radiopharm.*, 2018, **61**, 237–251.
- 13 X.-F. Wu, H. Neumann and M. Beller, *Chem. Rev.*, 2013, **113**, 1–35.
- 14 A. Brennfürher, H. Neumann and M. Beller, *Angew. Chem. Int. Ed.*, 2009, **48**, 4114–4133.
- 15 J. Magano and J. R. Dunetz, *Chem. Rev.*, 2011, **111**, 2177–2250.
- 16 C. Lescot, D. U. Nielsen, I. S. Makarov, A. T. Lindhardt, K. Daasbjerg and T. Skrydstrup, *J. Am. Chem. Soc.*, 2014, **136**, 6142–6147.
- 17 E. D. Hostetler and H. D. Burns, *Nucl. Med. Biol.*, 2002, **29**, 845–848.
- 18 M.-W. Wang, W.-Y. Lin, K. Liu, M. Masterman-Smith and C. K.-F. Shen, *Mol. Imaging*, 2010, **9**, 175–191.
- 19 K. Dahl, C. Halldin and M. Schou, *Clin. Transl. Imaging*, 2017, **5**, 275–289.
- 20 C.-C. Lee, *Science*, 2005, **310**, 1793–1796.
- 21 G. Pascali, P. Watts and P. A. Salvadori, *Nucl. Med. Biol.*, 2013, **40**, 776–787.
- 22 J. M. Gillies, C. Prenant, G. N. Chimon, G. J. Smethurst, W. Perrie, I. Hamblett, B. Dekker and J. Zweit, *Appl. Radiat. Isot.*, 2006, **64**, 325–332.
- 23 C. J. Steel, A. T. O'Brien, S. K. Luthra and F. Brady, *J. Label. Compd. Radiopharm.*, 2007, **50**, 308–311.
- 24 P. W. Miller, *J. Chem. Technol. Biotechnol.*, 2009, **84**, 309–315.
- 25 P. Watts, G. Pascali and P. A. Salvadori, *J. Flow Chem.*, 2012, **2**, 37–42.
- 26 H. Audrain, *Angew. Chem. Int. Ed.*, 2007, **46**, 1772–1775.
- 27 P. W. Miller, N. J. Long, A. J. de Mello, R. Vilar, H. Audrain, D. Bender, J. Passchier and A. Gee, *Angew. Chem. Int. Ed.*, 2007, **46**, 2875–2878.
- 28 S. Kealey, C. Plisson, T. L. Collier, N. J. Long, S. M. Husbands, L. Martarello and A. D. Gee, *Org. Biomol. Chem.*, 2011, **9**, 3313.
- 29 P. W. Miller, H. Audrain, D. Bender, A. J. deMello, A. D. Gee, N. J. Long and R. Vilar, *Chem. - Eur. J.*, 2011, **17**, 460–463.
- 30 K. Dahl, M. Schou, J. Ulin, C.-O. Sjöberg, L. Farde and C. Halldin, *RSC Adv.*, 2015, **5**, 88886–88889.
- 31 M. Ferrat, K. Dahl, C. Halldin and M. Schou, *J. Label. Compd. Radiopharm.*, DOI:10.1002/jlcr.3805.
- 32 T. Fukuyama, T. Totoki and I. Ryu, *Green Chem.*, 2014, **16**, 2042–2050.
- 33 Chemical Bonds and Bonds Energy - 2nd Edition, <https://www.elsevier.com/books/chemical-bonds-and-bonds-energy/sanderson/978-0-12-618060-2>, (accessed May 19, 2020).
- 34 J. C. Clark and P. D. Buckingham, *Int. J. Appl. Radiat. Isot.*, 1971, **22**, 639–646.
- 35 Y. Andersson and B. Langstrom, *J. Chem. Soc.-PERKIN Trans. 1*.
- 36 P. Lidström, T. Kihlberg and B. Långström, *J. Chem. Soc. Perkin 1*, 1997, 2701–2706.
- 37 An evaluation of a high-pressure ¹¹C carbonylation apparatus - Dahl - 2015 - Journal of Labelled Compounds and Radiopharmaceuticals - Wiley Online Library, <https://onlinelibrary.wiley.com/doi/full/10.1002/jlcr.3280>, (accessed June 29, 2020).
- 38 S. K. Zeisler, M. Nader, A. Theobald and F. Oberdorfer, *Appl. Radiat. Isot.*, 1997, **48**, 1091–1095.
- 39 Reduction of [¹¹C]CO₂ to [¹¹C]CO using solid supported zinc - Dahl - 2017 - Journal of Labelled Compounds and Radiopharmaceuticals - Wiley Online Library, <https://onlinelibrary.wiley.com/doi/full/10.1002/jlcr.3561>, (accessed June 29, 2020).
- 40 W. Zhang, Y. Hu, L. Ma, G. Zhu, Y. Wang, X. Xue, R. Chen, S. Yang and Z. Jin, *Adv. Sci.*, 2018, **5**, 1700275.
- 41 K. Li, X. An, K. H. Park, M. Khraisheh and J. Tang, *Catal. Today*, 2014, **224**, 3–12.
- 42 D. U. Nielsen, X.-M. Hu, K. Daasbjerg and T. Skrydstrup, *Nat. Catal.*, 2018, **1**, 244–254.
- 43 G. Zhao, X. Huang, X. Wang and X. Wang, *J Mater Chem A*, 2017, **5**, 21625–21649.
- 44 B. Kumar, M. Llorente, J. Froehlich, T. Dang, A. Sathrum and C. P. Kubiak, *Annu. Rev. Phys. Chem.*, 2012, **63**, 541–569.
- 45 B. Endrődi, G. Bencsik, F. Darvas, R. Jones, K. Rajeshwar and C. Janáky, *Prog. Energy Combust. Sci.*, 2017, **62**, 133–154.
- 46 A. Fridman, *Plasma Chemistry*, Cambridge University Press, Cambridge, 2008.
- 47 R. Aerts, W. Somers and A. Bogaerts, *ChemSusChem*, 2015, **8**, 702–716.
- 48 H. V. Boenig, *Fundamentals of plasma chemistry and technology*, Technomic Pub. Co., Lancaster, 1988.
- 49 D. S. Laitar, P. Müller and J. P. Sadighi, *J. Am. Chem. Soc.*, 2005, **127**, 17196–17197.
- 50 C. Kleeberg, M. S. Cheung, Z. Lin and T. B. Marder, *J. Am. Chem. Soc.*, 2011, **133**, 19060–19063.
- 51 M. Flinker, S. Lopez, D. Nielsen, K. Daasbjerg, F. Jensen and T. Skrydstrup, *Synlett*, 2017, **28**, 2439–2444.
- 52 M. S. Moss, K. Yanallah, R. W. K. Allen and F. Pontiga, *Plasma Sources Sci. Technol.*, 2017, **26**, 035009.

- 53 U. Kogelschatz, B. Eliasson and W. Egli, *J. Phys. IV*, 1997, **07**, C4-47-C4-66.
- 54 Wengler J, Ognier S, Al Ayoubi S, Tatoulian M (2019) Biphasic Plasma Microreactor and Method of Using the Same, WO/2019/166570
- 55 J. Wengler, S. Ognier, M. Zhang, E. Levernier, C. Guyon, C. Ollivier, L. Fensterbank and M. Tatoulian, *React. Chem. Eng.*, 2018, **3**, 930–941.
- 56 M. Zhang, S. Ognier, N. Touati, I. Hauner, C. Guyon, L. Binet and M. Tatoulian, *Plasma Process. Polym.*, 2018, **15**, 1700188.
- 57 A. Lepoetre, S. Ognier, M. Zhang, J. Wengler, S. Al Ayoubi, C. Ollivier, L. Fensterbank, X. Duten, and M. Tatoulian, *Plasma Processes And Polymers*, 2020, under review
- 58 M. Ramakers, I. Michielsen, R. Aerts, V. Meynen and A. Bogaerts, *Plasma Process. Polym.*, 2015, **12**, 755–763.
- 59 M. A. Lindon and E. E. Scime, *Front. Phys.*, , DOI:10.3389/fphy.2014.00055.
- 60 J. S. Moore, C. D. Smith and K. F. Jensen, *React. Chem. Eng.*, 2016, **1**, 272–279.
-